JOTCS A
Journal of the Turkish Chemical Society
Section: A
Chemistry
TURKISH CHEMICAL SOCIETY

Probing the Electro-Chemical and Thermal Properties of Polyaniline/MWCNT Nanocomposites

Sharon J. Paul[1], Sarvesh Kumar Singh[1], Jaya Tuteja[2], Arpit Sand[2], and Prakash Chandra[1*]

[1]Bundelkhand University, Department of Chemistry, Jhansi, Uttar Pradesh, 284128, India
[2]Manav Rachna University Department of Chemistry, Faridabad, 121004, India

Abstract: The tremendous interest for robust, clean energy storage devices to comprehend the growing needs of modern gadgets has led to exploration of materials having unprecedented electrochemical and interfacial properties. Here, the present study deals with the synergistic effects of multi walled carbon nanotubes and polyaniline nanocomposites on the electro-chemical and thermal properties for wide-range of applications. The microstructural, structural, and optical characterizations have been evaluated through scanning electron microscopy (SEM), transmission electron microscopy (TEM), X-ray diffraction (XRD), Fourier transform infrared spectroscopy (FTIR), and UV-Vis spectrophotometry. The thermal stability of the product was also studied through thermal gravimetric analysis (TGA) and the room temperature electrical conductivity was also measured. An exceptional enhancement in thermal stability and conductivity has been observed apparently due to interfacial properties of polyaniline (PANI) and multiwalled carbon nanotubes (MWCNTs). Further, in present study we are going to report a comparative analysis of thermal and electrical properties of PANI/MWCNT nanocomposites with different loadings of MWCNTs. The room temperature conductivity as calculated for 1%, 2%, 4% and 8% MWCNT loading is around 2.019, 3.075, 4.48, 8.73 S/cm respectively. The mechanism for thermal and electrical enhancements in PANI-coated MWCNT nanocomposites is also expounded.

Keywords: Nanocomposites, MWCNTs, polyaniline, nanotechnology, polymer nanocomposites

Submitted: September 19, 2022. **Accepted:** April 24, 2023.

Cite this: Paul SJ, Singh SK, Tuteja J, Sand A, Chandra P. Probing the Electro-Chemical and Thermal Properties of Polyaniline/MWCNT Nanocomposites. JOTCSA. 2023;(2):493–504.

DOI: https://doi.org/10.18596/jotcsa.1177040.

***Corresponding author. E-mail:** drprakashcy@gmail.com

1. INTRODUCTION

The advent of nanoscience and nanotechnology has prompted the use of polymer matrix nanocomposites since past few decades. The polymer nanocomposite consists of a polymer guest matrix reinforced with fillers with dimensions in nano-regime. Polymer nanocomposites are an innovative class of uniquely modified materials that come into existence due to the extraordinary collaborations of properties like electrical, magnetic, catalytic, mechanical, biodegradability, etc. between the polymer and nanofiller. Polymer nanocomposites are preferred over metal matrix composites and ceramic matrix composites as they require relatively low processing temperatures for fabrication. Moreover, the polymer matrix also assists to transfer stress through the medium by equally distributing the applied load within the composite (1). Polymer matrix nanocomposites have extensively been investigated the class of intrinsically conducting polymers (ICPs) owing to their intriguing redox and electronic properties (2,3). Carbon nanotubes (CNTs) are viewed as effective reinforcements to produce unique composite materials with novel properties for nano-scale engineering applications.

The dedicated literature studies has revealed that the combination of conducting polymers and

nanomaterials offers an opportunity to improve the mechanical, electrical, and thermal properties, along with introduction of new electronic properties based on interactions between the two compounds. Low density polyethylene nanocomposites incorporated with silicon dioxide nanoparticles (LDPE/SiO_2) have demonstrated high tolerance to the worst conditions when used as high-voltage insulation systems with enhanced thermal and mechanical properties (4). Nanocomposites of polyvinyl chloride (PVC) with titanium oxide (TiO_2) nanoparticles, and LPDE/PVC nanocomposites have been used in power cable insulation with improved electric and dielectric properties (5,6).

Polyaniline (PANI) is considered as the best ICP in terms of technological and commercial aspects. It surpasses other conducting polymers owing to high conductivity (7), better environmental stability (8), unique electro chemical properties (9), availability of cheap monomer (10) and facile synthesis technique (11). Since ever the discovery of CNTs (12) their exceptional, electrical, thermal and mechanical properties (13,14) have made them a vital contributor in vast applications. The inclusion of CNTs as conductive fillers in reinforced PANI matrix gives rise to polymer nanocomposites with new synergies possessing enhanced conductivity, improved thermal and electrical properties, and such a nanocomposite could be deployed for fuel cell (15), solar cell (16), supercapacitor (17), EMI shielding (18), gas sensor (19), and battery materials (20). There have been studies on the potential applications of polyaniline-multi walled carbon nanotubes (PANI/MWCNT) nanocomposites for EMI shielding, supercapacitor, sensors and solar cells. Manganese dioxide, multi walled carbon nanotubes incorporated polyaniline (MnO_2/PANI/MWCNT) nanocomposite showed a specific capacitance of 395.0 $F \cdot g^{-1}$ with 72% consistency over 1000 charge-discharge cycles and capability to be used as an electrode material for supercapacitors (21). PANI/MWCNT composites have also been successfully used in real sample detection and analysis of liquid ammonia (22). PANI/MWCNT/thermally annealed graphene/aerogel/epoxy nanocomposites have shown high efficiency for electromagnetic interference shielding applications with 52.1 S/cm electrical conductivity and 171.3 °C heat resistance index (T_{HRI}) (23). PANI/MWCNT have also shown high microwave absorbing performance when MWCNTs were modified with magnetic nanoparticles of ferric oxide and ferrous oxide (24). The day-by-day progression of CNT-assisted polymeric devices in nano-electronics requires a comprehensive concept and better understanding of the electrical attributes of nanocomposites of PANI and MWCNTs. The present study focuses on a comparative analysis of thermal and electrical properties with different MWCNT loadings that could be helpful to synthesize desired composite for different applications and encourage future studies. Although several efforts have been made in this area yet there is a scope of finding a suitable material whose distinctive properties are not compromised and are stable under ambient conditions. PANI/MWCNT nanocomposites could prove to be the ultimate materials with lightweight and high stability as MWCNTs have high surface area and porosity, and are extremely light-weighted.

Herein, we report the in-situ oxidative polymerization of aniline monomer with surfactant assisted dispersion of MWCNTs to obtain PANI/MWCNT nanocomposites with better performance and profound enhancements in thermal, electrical properties as compared to the original materials. A number of parameters, surface morphology, tunable properties of PANI/MWCNT nanocomposites with different MWCNT loadings, and their correlation with the thermal and electrical properties are investigated. We give an account on the potential of PANI/MWCNT nanocomposite with different MWCNT loadings to expand the known literature and provide better understanding for futuristic studies.

2. MATERIALS AND METHODS

2.1. Materials

MWCNTs were produced in laboratory *via* chemical vapor deposition (CVD) method. The precursors essential for synthesis of nanocomposites *i.e* the monomer aniline was procured from E-Merck India Ltd., potassium persulfate (PPS) was used as an oxidant, cetyl-trimethyl ammonium bromide (CTAB) as a surfactant, HCl to prepare the molar solution and ethanol used for washing the nanocomposites were procured from CDH India Ltd. The water used in the experiments is de-ionized water (DI). All chemicals used are of analytical reagent (AR) grade.

2.2. Synthesis of MWCNTs

MWCNTs were synthesized by CVD process and its average length was ~250 µm and diameter was ~28 nm as reported in our previous work (25). Briefly, ferrocene was dissolved in xylene in a particular ratio. Here, ferrocene was required to obtain Fe catalyst particles and xylene was used for carbon source. This liquid feed was kept in a quartz tube that was placed in the tube furnace. One end of the quartz tube was connected to a bladder in order to collect the exhaust gases while the other end was closed. The tube furnace was kept under argon flow and heated at around 650-800 °C. After achieving the final reaction temperature, the furnace was maintained at that temperature for 30 min and then the reactor was allowed to cool to room temperature. The growth of MWCNTs occurred on surfaces inside the quartz tube.

2.3. Synthesis of PANI/MWCNT Nanocomposites

PANI/MWCNTs nanocomposites were synthesized *via* in situ oxidative polymerization of aniline monomer in the presence of an oxidizing agent and a surfactant. PPS was used as the oxidizing agent and

CTAB was used as a surfactant. Primarily, 1 M HCl stock solution of aniline and PPS were prepared, labeled as solution A (aniline in 1 M HCl) and solution B (PPS in 1 M HCl). The molar ratio of aniline: PPS: CTAB was kept as 1: 0.5: 1. Due to low dispersity of MWCNTs, ultrasonication technique and surfactant was used. Well-dispersed suspension of MWCNTs with different amounts of MWCNTS *i.e*, 1%, 2%, 4%, and 8% in 1 M HCl solution using CTAB and ultrasonication were obtained. This MWCNT solution was added to solution A on constant stirring. Later, solution B was added slowly, dropwise to the dispersion of MWCNTs and solution A to polymerize aniline monomer. The MWCNTs are mixed in the course of the polymerization process, to ensure uniform distribution and homogeneous coating of PANI over MWCNTs. The reaction mixture was kept on constant agitation on magnetic stirrer for 24 hrs and it gradually turned into greenish black slurry. It was then filtered through vacuum filtration and the residue was repeatedly washed with DI water and ethanol via centrifugation in order to remove the unreacted oligomers or the residual impurities. The as-synthesized PANI/MWCNTs nanocomposites with different MWCNT content were dried at 60 °C in air oven, then ground into fine powder with the help of a motor-powered pestle. Pure polyaniline was also synthesized in the same manner without the use of surfactant and MWCNTs. The reason for selecting HCl as the stock solution medium rather than any other protic acid is clearly indicated in our previous work (25). The optical images of as-synthesized powdered PANI/MWCNT nanocomposite and dispersion of PANI/MWCNT nanocomposite is shown in Figure S1.

2.4. Measurements

X-ray diffraction (XRD) patterns were recorded in the 2θ range from 10 to 60 degrees through Rigaku: MiniFlex, CuKα1; λ = 1.5406 Å. The structural examination was performed with the help of SEM-EVO SEM MA15/18 and TEM - Tecnai G20-twin, 200 kV with super twin lenses having 0.144 nm point and 0.232 nm line resolution, respectively. FTIR studies were performed using a Perkin Elmer 3725 instrument from 400 cm^{-1} to 4000 cm^{-1} and UV–Vis absorption studies were performed using a Shimadzu UV−1601 spectrophotometer which is calibrated and traceable with the standard sample of Rhodamine B. The TGA studies were carried out under N_2 atmosphere (flow of 100 mL/min) from 24 °C to 700 °C at 10 °C/min, by Thermal Analysis Modulus, SDT Q600 (TA Instruments) controlled through Q Series software.

3. RESULTS AND DISCUSSION

Intrinsically conducting polymer-based nanocomposites with PANI matrix and MWCNTs as efficient reinforced conductive fillers have been synthesized with 1%, 2%, 4%, and 8% MWCNT loadings. The characterization and property determination parameters reveal that PANI/MWCNT nanocomposites have improved thermal and electrical properties when compared to the pristine polymer.

3.1. Structural and Microstructural Studies

The structural studies and microstructural studies were achieved through XRD, SEM, and TEM. The characteristic peaks of PANI appears at around 2θ values of 15°, 20°, and 25°, corresponding to (011), (020) and (200) crystal planes of PANI (26) as shown in supplementary information Figure S2. These peaks arise due to chain propagation by sequential addition of aniline monomers. The pure MWCNT in Figure S3 exhibits a sharp peak at around 2θ value of 26° that correlates to the (002) planes of MWCNT whereas the peaks at around 43° correspond to the (110) and (100) graphitic planes and small amount of catalytic Fe particles incorporated in the walls of MWCNTs during synthesis (27). PANI/MWCNT nanocomposites in Figure 1 show similar crystalline behavior as that of polyaniline. The intense peak at around 25° is the superimposed peak of MWCNTs and PANI. The peaks in the nanocomposites are more prominent with increased peak intensity as compared to pure polyaniline. This is due to the encapsulation of MWCNTs and ordering of PANI along the MWCNT axis (28). However, the peaks of MWCNTs at around 43° fade away in the diffractograms of PANI/MWCNT nanocomposites implying that the MWCNTS are coated effectively by PANI and covalent interactions between the phases is absent (29). It can be inferred that better dispersion of MWCNTs in the PANI polymer matrix improves the crystallinity of the nanocomposites.

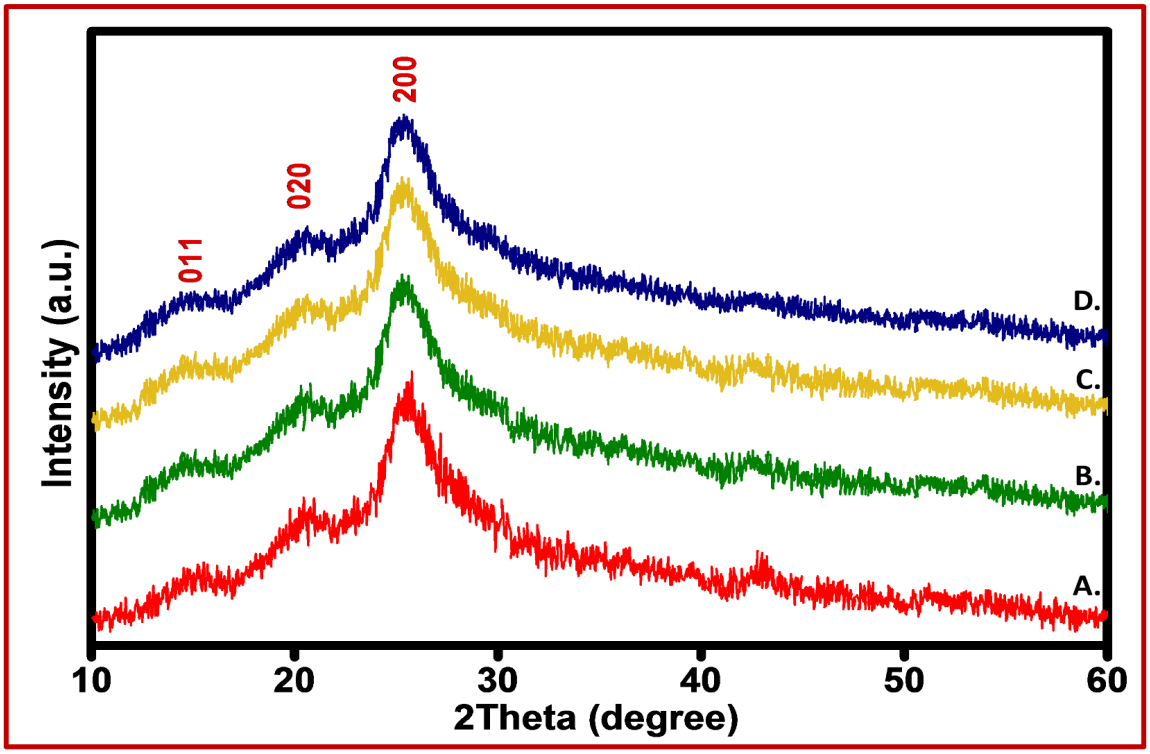

Figure 1: XRD patterns of (A) PANI@1%MWCNT nanocomposite, (B) PANI@2%MWCNT nanocomposite, (C) PANI@4%MWCNT nanocomposite and (D) PANI@8%MWCNT nanocomposite.

The morphology of the as-synthesized PANI/MWCNT nanocomposites was examined by SEM. The homogeneous dispersion of MWCNTs in PANI is clearly discernible from Figure 2, indicating that MWCNTs are well coated by the polymer. Some interwoven fibrous structures are visible that act as a conductive network to facilitate high conductivity as compared to pure PANI. These compatible interactions between MWCNTs and PANI improve the charge transfer process thereby influencing the charge transport properties of the nanocomposites. The highly agglomerated smooth globular morphology of pure PANI is visible in Figure S4. Thereby the increased diameter and rough surface of the tubular structures in the nanocomposites indicate effective polymer coating over the MWCNTs. The micrographs also show a systematic change in morphology of the nanocomposites that with the increase of MWCNTs content the globular structures change to more uniformly coated tubular structures.

To visualize the microstructure more clearly and to support the tubular morphology withdrawn from SEM, HRTEM was also performed. The HRTEM micrographs of PANI/MWCNT nanocomposites are revealed in Figure 3. The surface morphology is tubular and suggests that aniline has undergone polymerization over the MWCNTs core. The interconnected fibrous structures are also clearly visible.

Raman spectra were also used to examine the effect of interaction of PANI and MWCNTs on the structure of the nanocomposites. The Raman studies of PANI and PANI/MWCNT nanocomposite both show characteristic D-band at around 1365 cm^{-1} and G-band at around 1570 cm^{-1}. The D-band corresponds to the disordered graphite structure and structural intensity of sp^3 hybridized carbon atoms. The G-band is attributed to the structural intensity of the sp^2 hybridized carbon atoms and the D/G ratio is used to determine the degree of defects on MWCNTs. The Raman spectra of PANI and PANI/MWCNT nanocomposite in Figure S5 show no significant difference in D/G ratio, therefore indicating that no defects are created on the surface of MWCNTs during the process of polymerization. This also reveals that the interactions are purely physical in nature.

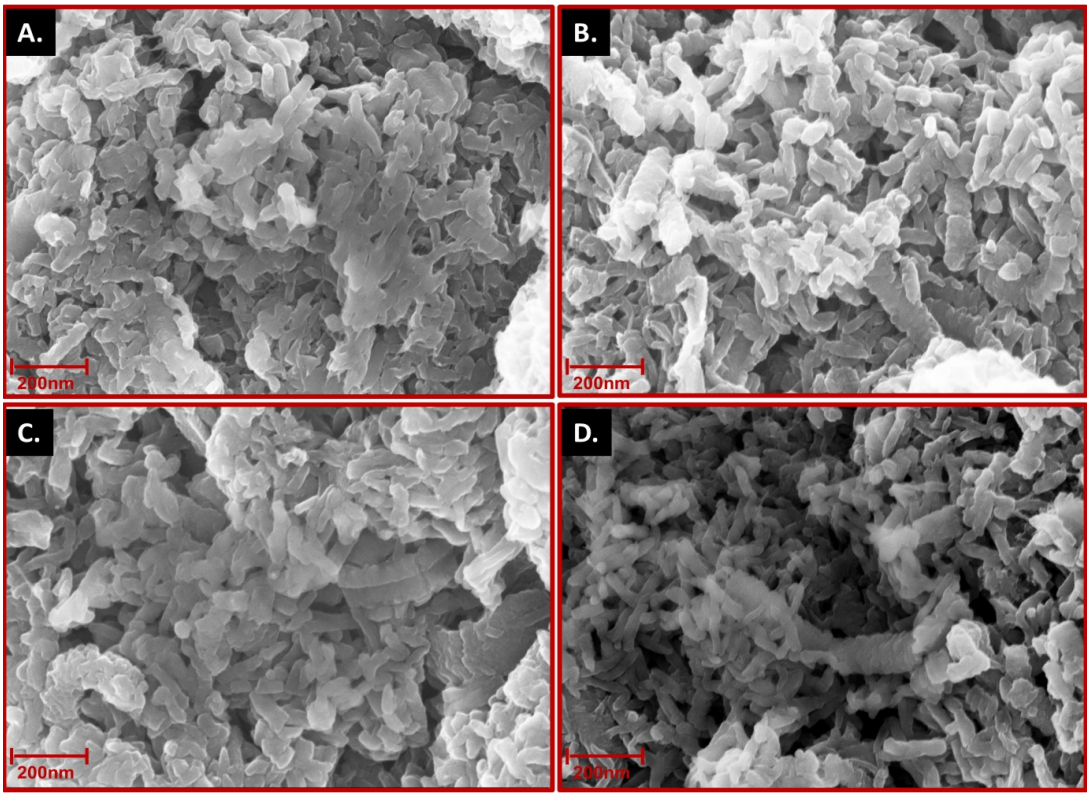

Figure 2: SEM images of (A) PANI@1%MWCNT nanocomposite, (B) PANI@2%MWCNT nanocomposite, (C) PANI@4%MWCNT nanocomposite, and (D) PANI@8%MWCNT nanocomposite.

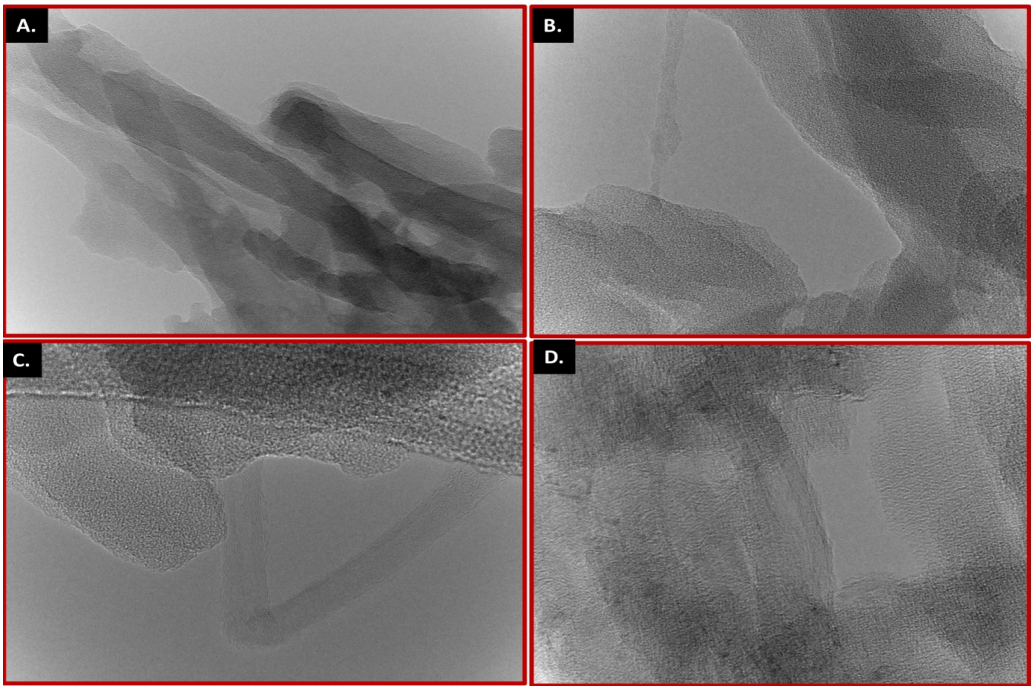

Figure 3: HRTEM images of (A) PANI@1%MWCNT nanocomposite, (B) PANI@2%MWCNT nanocomposite, (C) PANI@4%MWCNT nanocomposite and (D) PANI@8%MWCNT nanocomposite.

3.2. FT-IR Studies

Optical studies were performed to understand the polymer backbone of the polymer nanocomposites and it includes FT-IR and UV-vis spectroscopy. FT-IR spectroscopy helps to elucidate the nature of the interaction amongst PANI and MWCNT and identify the functionalities. Figure 4 depicts the FTIR spectra of PANI/MWCNT nanocomposites. The main characteristic peak of PANI at around 3404 cm^{-1} is associated to the N-H stretching vibration (27). The peak at around 2942 cm^{-1}, 2837 cm^{-1} is due to the asymmetric stretching of CH and symmetric stretching of C-H. The peak at around 1575 cm^{-1} is assigned to C=C stretching mode of the quinoid rings, 1452 cm^{-1} is due to C=C stretching mode of benzenoid rings and the peak at around 1380 cm^{-1} can be related to C-N stretching mode. The peak at around 1050 cm^{-1} and 880 cm^{-1} is attributed to the in-plane and out-of-plane bending vibration of C-H of 1, 4-disubstituted benzenoid ring. Thus it can be inferred that the incorporation of MWCNTs did not affect the polymer backbone. All the obtained peaks were similar as those studied in the literature (30,31) and confirmed the formation of the PANI and its nanocomposites.

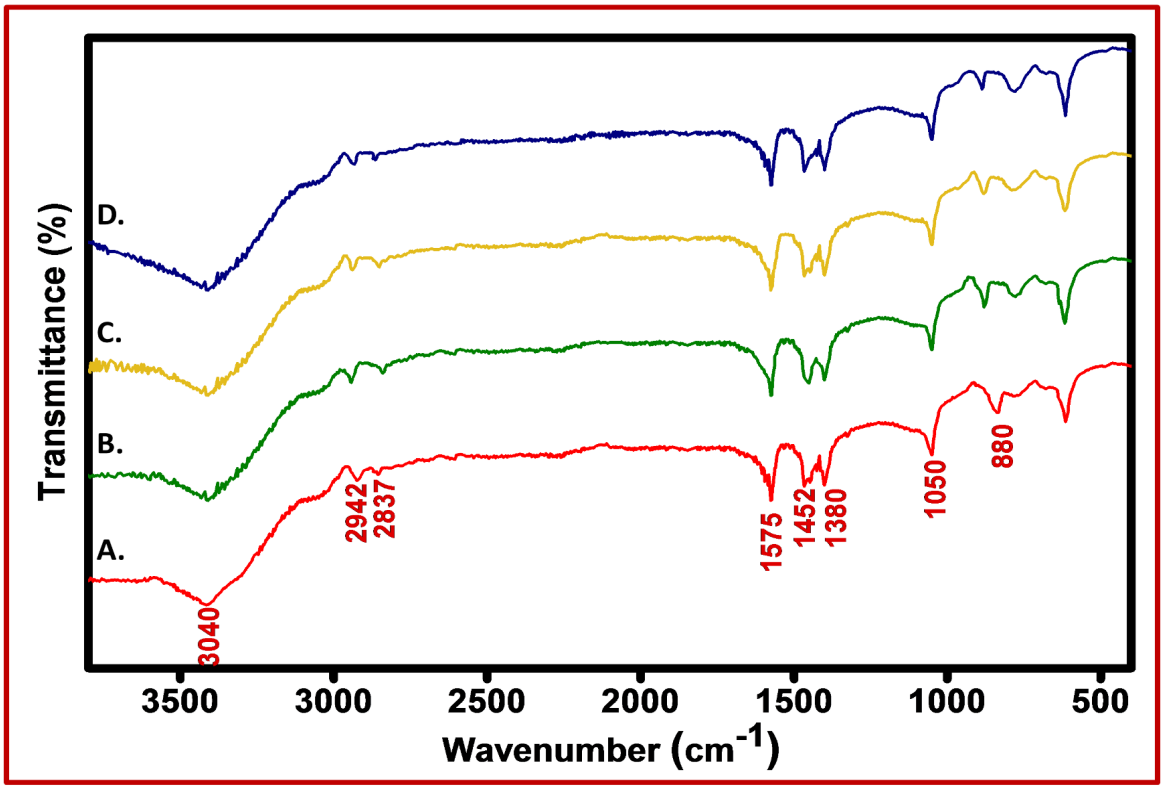

Figure 4: FT-IR spectra of (A) PANI@1%MWCNT nanocomposite, (B) PANI@2%MWCNT nanocomposite, (C) PANI@4%MWCNT nanocomposite and (D) PANI@8%MWCNT nanocomposite.

3.3. UV-Vis Studies

To comprehend the effect of MWCNTs filler on PANI backbone more efficaciously, UV–Vis spectroscopy was performed on all samples. Figure 5 shows the UV-Vis spectra of PANI/MWCNT nanocomposites. The UV-Vis spectrum of PANI in Figure S6 shows absorption peaks at around 342 nm, 435 nm and 860 nm (32). The small absorption peak at around ~342 nm is ascribed to π→π* transition of the benzenoid rings and the shoulder at around ~435 nm signifies polaronic peak indicating the protonation of the polymer and the broad shoulder at ~860 nm shows free carrier tail, which confirms that the presence of MWCNT kept the polymer backbone intact. The PANI/MWCNT nanocomposites demonstrated these characteristic absorption bands but there is a hypsochromic shift of π→π* band. The band which appears at nearly 342 nm in PANI appears at 335 nm, 332, 329 nm, 326 nm in PANI/MWCNT nanocomposites with 1%, 2%, 4% and 8% MWCNTs content. This shift in the *π–π** electronic transition towards shorter wavelength with the addition of the MWCNTs is due to site-selective interactions amongst the quinoid units of PANI and MWCNTs (33, 34). Along with it, the polaronic peaks undergo bathochromic shift as compared to pristine PANI, indicating higher conductivity as the bipolaron/polaron assists in charge transfer processes.

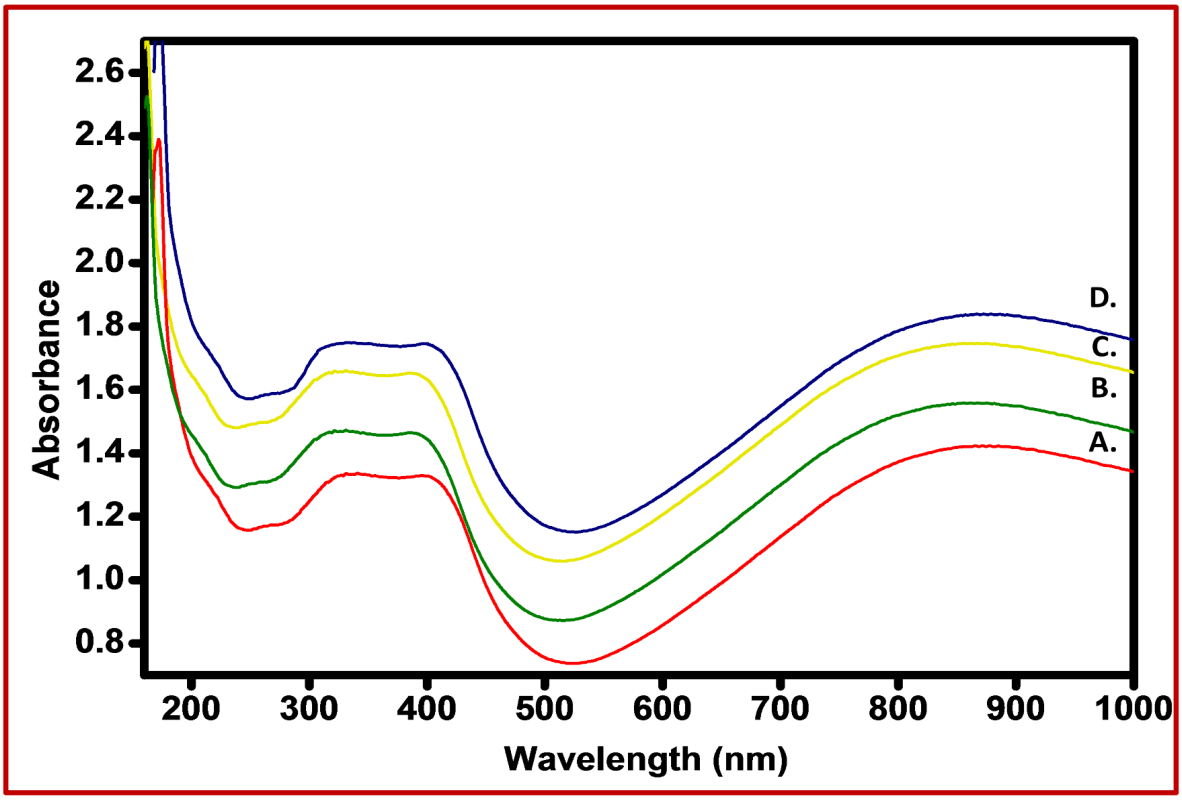

Figure 5: UV-Vis of (A) PANI@1%MWCNT nanocomposite, (B) PANI@2%MWCNT nanocomposite, (C) PANI@4%MWCNT nanocomposite and (D) PANI@8%MWCNT nanocomposite.

3.4. Thermal Analysis

TGA measurement was carried on the nanocomposites to determine the thermal stability enhancements in the nanocomposites after the addition of MWCNTs. This measurement also proved useful to evaluate the maximum possible temperature to endorse the suitable thermal range of the nanocomposites. The thermograms of PANI/MWCNT nanocomposites are shown in Figure 6 and pure PANI is shown in Figure S7. The samples are heated from room temperature up to 700˚C. In pure PANI approximately 15–18 % of weight loss occurs as a consequence of loss of water molecules at around 25˚C until 100˚ C. A slight weight loss is attained up to 400 °C and thereafter a rapid weight loss occurs due to the degradation of the polymer chain. In the case of PANI/MWCNT nanocomposites, the first step weight loss occurs till 100 °C due to loss of water molecules and the second step weight loss occurs till 200 °C due to elimination of dopant. The third step weight loss occurs from 300 °C to 500 °C which involves slow and steady degradation of polymer backbone. The final rapid weight loss occurs due to the complete breakdown of polymer chain till 700 °C. The remaining 30-40% weight left is the char residues of inert materials like the MWCNTs, Fe-catalyst, and some carbonized specks of polymer chain. The thermograms reveal that the thermal stability enhances with the increase in the MWCNTs content. The surface interactions between MWCNTs and PANI increases the thermal stability of the polymer blend, in other words, MWCNTs reduce the mass loss (35, 36). The thermal degradation of PANI is a complex chain process consisting of chain reactions that produce additional active intermediates. MWCNT break these chains at higher temperatures and increase thermal stability and reducing the initial fragmentation of polymer chain. They also indicate significantly enhanced thermal stability of the nanocomposite than that of pure PANI.

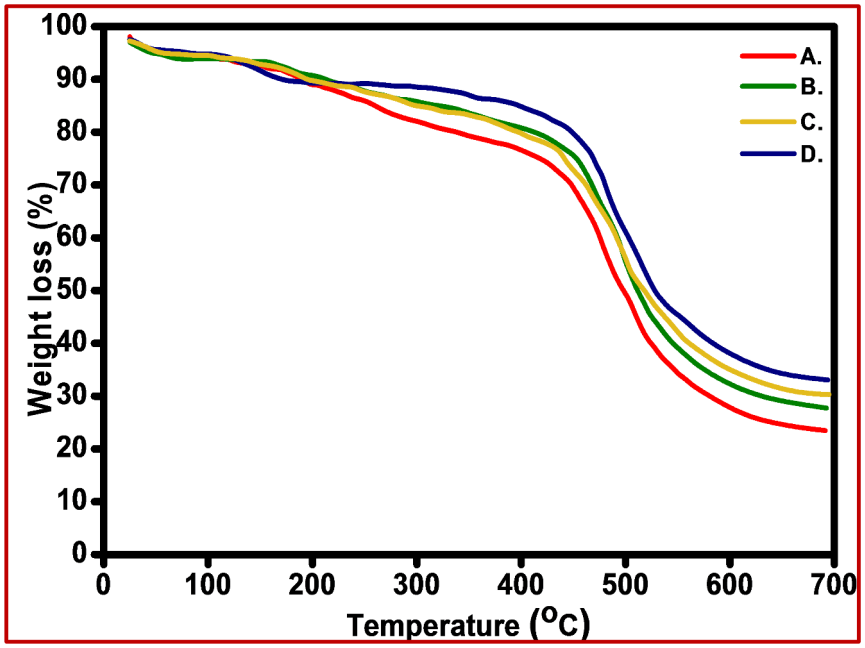

Figure 6: TGA curves of (A) PANI@1%MWCNT nanocomposite, (B) PANI@2%MWCNT nanocomposite, (C) PANI@4%MWCNT nanocomposite and (D) PANI@8%MWCNT nanocomposite.

3.5. Conductivity

The conductivity of the nanocomposites was determined at room temperature. To perform the measurements pellets of approximately the same thickness were made with the help of hydraulic press under identical conditions. Then silver paste was applied on both sides of the pellet to establish contacts for the measurement of bulk resistance. The conductivity was then calculated using the resistance and thickness of pellet through the following equation:

$$\sigma = L/RA$$

where “σ” denotes the conductivity ,“L” denotes the length of the pellet, “R” represents resistance and “A” denotes the cross sectional area of the pellets.

There is continuous increase in conductivity with the increase in the MWCNT content. Such high conductivities of the nanocomposites is attributed to core shell structure, where the micrometer long MWCNTs as core are effectively coated with PANI as shell which is clearly evident from the SEM images. The effectively interacting interface helps to facilitate charge transfer process between the MWCNTs and the conducting emeraldine salt of PANI. MWCNTs prove to be the conducting bridge owing to their extremely conducting behavior and high aspect ratio, joining the PANI individual structures coated over MWCNTs. This further upsurges the coupling amongst the polymer chains and induces enhancements in inter-chain charge transport. This synergistic effect of the two compatible components, PANI and MWCNT leads to raised conductivity of the nanocomposite which is much more than the pure polymer itself thereby profusely improving the electrical properties.

In order to understand the conduction mechanism it is important to understand the structure of both components. In PANI each carbon atom contains an unpaired (π) electron, these electrons overlap and generate charge delocalization over the polymer backbone, creating a pathway for charge mobility throughout the polymer chain (37). This conduction pathway plays a vital role. PANI is conductive in its emeraldine salt state, which is formed by the protonation of the imine group by doping them with acids. This initially form an intermediate bipolar on state by successive rearrangements and then forms a polaron (38, 39). Moreover, MWCNTs being excellent electron acceptors and PANI being a relatively good electron donor, form π- π * between the MWCNTs surface and quinoid unit of PANI (40). It is important to note that undoped form of PANI, *i.e* emeraldine base, which acts as an insulator, has no charge transfer systems in the polymer backbone, thus prohibiting its interaction with MWCNTs (41).

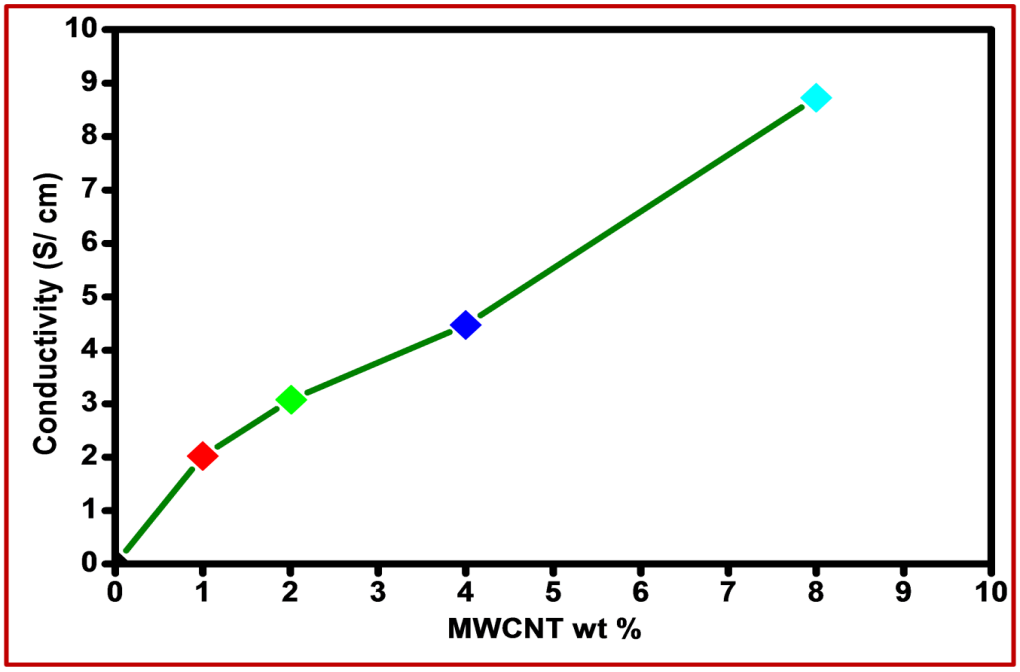

Figure 7: Variation of room temperature conductivity of PANIMWCNT nanocomposites with different MWCNT loadings.

4. CONCLUSION

In the present investigation, PANI/MWCNT nanocomposites with different MWCNTs loading were synthesized by *in-situ* oxidative polymerization. The tubular morphologies of the nanocomposites revealed the core shell structure of homogeneous coating of PANI over MWCNTs. Several parameters were analyzed before deploying the nanocomposites for application perspective. The synergistic effects of PANI and MWCNTs greatly related to the profound enhancements in thermal stability and conductivity of the nanocomposites, thereby keeping the polymer backbone undamaged. The FTIR spectrum that showed the decreased benzoid to quinoid intensity ratio and the blue shift in the π–π *electronic transition in the case of the UV spectrum also confirmed the interaction between the PANI and the MWCNTs. This study suggests that PANI/MWCNT nanocomposites are better electronic materials than pristine PANI, and on increasing the concentration of MWCNTs in PANI changes the behavior of PANI from that of a semiconductor to a metal. Further, as MWCNT doping is increased the thermal stability and conductivity of the PANI/MWCNT nanocomposites is enhanced manifolds.

5. CONFLICT OF INTEREST

The authors declare that the research was conducted in the absence of any commercial or financial relationships that could be construed as a potential conflict of interest.

6. ACKNOWLEDGMENTS

S.J.P would also like to acknowledge DST for providing the funding under INSPIRE-Fellowship Scheme (IF 160064).

7. SUPPLEMENTARY MATERIAL

Supplementary data related to this article consist of XRD patterns of PANI and MWCNT, SEM image of PANI, Raman spectra of PANI and PANI/MWCNT nanocomposite, UV-Vis of PANI, and TGA curve of PANI.

8. REFERENCES

1. Khalil HA, Fizree H, Bhat A, Jawaid M, Abdullah C. Development and characterization of epoxy nanocomposites based on nano-structured oil palm ash. Composites Part B: Engineering. 2013;53:324-33. <URL>

2. Jaymand M. Recent progress in chemical modification of polyaniline. Progress in Polymer Science. 2013;38(9):1287-306. <URL>

3. Bhadra S, Khastgir D, Singha NK, Lee JH. Progress in preparation, processing and applications of polyaniline. Progress in Polymer Science. 2009;34(8):783-810. <URL>

4. Darwish M, Ahmed HM, Mansour D-EA, editors. Thermo-mechanical properties of LDPE/SiO 2 nanocomposites based on chemically functionalized SiO 2 nanoparticles. International Symposium on Electrical Insulating Materials (ISEIM); 2020: IEEE. 241-244. <URL>

5. Abdel-Gawad NM, El Dein AZ, Mansour DEA, Ahmed HM, Darwish MM, Lehtonen M. PVC nanocomposites for cable

insulation with enhanced dielectric properties, partial discharge resistance and mechanical performance. High Voltage. 2020;5(4):463-71. <URL>

6. Mansour D-EA, Abdel-Gawad NM, El Dein AZ, Ahmed HM, Darwish MM, Lehtonen M. Recent advances in polymer nanocomposites based on polyethylene and polyvinylchloride for power cables. Materials. 2020;14(1):66. <URL>

7. Stejskal J, Gilbert R. Polyaniline. Preparation of a conducting polymer (IUPAC technical report). Pure and applied chemistry. 2002;74(5):857-67. <URL>

8. Chiang JC, Macdiarmid AG. Polyaniline - protonic acid doping of the emeraldine form to the metallic regime. Synthetic Metals. 1986;13(1-3):193-205. <URL>

9. Kobayashi T, Yoneyama H, Tamura H. Polyaniline film-coated electrodes as electrochromic display devices. Journal of Electroanalytical Chemistry. 1984;161(2):419-23. <URL>

10. Genies EM, Boyle A, Lapkowski M, Tsintavis C. Polyaniline - a historical survey. Synthetic Metals. 1990;36(2):139-82. <URL>

11. Macdiarmid AG, Chiang JC, Halpern M, Huang WS, Mu SL, Somasiri NLD, et al. Polyaniline - Interconversion of Metallic and Insulating Forms. Molecular Crystals and Liquid Crystals. 1985;121(1-4):173-80. <URL>

12. Iijima S, Ichihashi T. Single-shell carbon nanotubes of 1-nm diameter. Nature. 1993;363(6430):603-5. <URL>

13. Baughman RH, Zakhidov AA, de Heer WA. Carbon nanotubes - the route toward applications. Science. 2002;297(5582):787-92. <URL>

14. Fischer JE, Dai H, Thess A, Lee R, Hanjani NM, Dehaas DL, et al. Metallic resistivity in crystalline ropes of single-wall carbon nanotubes. Physical Review B. 1997;55(8):R4921-R4. <URL>

15. Wang Y, Chen Y, Wen Q, Zheng H, Xu H, Qi L. Electricity generation, energy storage, and microbial-community analysis in microbial fuel cells with multilayer capacitive anodes. Energy. 2019;189:116342. <URL>

16. Zhang H, He B, Tang Q, Yu L. Bifacial dye-sensitized solar cells from covalent-bonded polyaniline–multiwalled carbon nanotube complex counter electrodes. Journal of Power Sources. 2015;275:489-97. <URL>

17. Al-badri M, Albdiry M. Electrochemical performance of ternary s-GN/PANI/CNTs nanocomposite as supercapacitor power electrodes. Periodicals of Engineering and Natural Sciences. 2020;8(4):2484-9. <URL>

18. Zou L, Lan C, Yang L, Xu Z, Chu C, Liu Y, et al. The optimization of nanocomposite coating with polyaniline coated carbon nanotubes on fabrics for exceptional electromagnetic interference shielding. Diamond and Related Materials. 2020;104:107757. <URL>

19. Roy A, Ray A, Sadhukhan P, Naskar K, Lal G, Bhar R, et al. Polyaniline-multiwalled carbon nanotube (PANI-MWCNT): Room temperature resistive carbon monoxide (CO) sensor. Synthetic Metals. 2018;245:182-9. <URL>

20. Wang CY, Mottaghitalab V, Too CO, Spinks GM, Wallace GG. Polyaniline and polyaniline–carbon nanotube composite fibres as battery materials in ionic liquid electrolyte. Journal of Power Sources. 2007;163(2):1105-9. <URL>

21. Huang Y, Lu J, Kang S, Weng D, Han L, Wang Y. Synthesis and application of MnO2/PANI/MWCNT ternary nanocomposite as an electrode material for supercapacitors. Int J Electrochem Sci. 2019;14:9298-310. <URL>

22. Maity D, Manoharan M, Kumar RTR. Development of the PANI/MWCNT Nanocomposite-Based Fluorescent Sensor for Selective Detection of Aqueous Ammonia. Acs Omega. 2020;5(15):8414-22. <URL>

23. Huangfu Y, Ruan K, Qiu H, Lu Y, Liang C, Kong J, et al. Fabrication and investigation on the PANI/MWCNT/thermally annealed graphene aerogel/epoxy electromagnetic interference shielding nanocomposites. Composites Part A: Applied Science and Manufacturing. 2019;121:265-72. <URL>

24. Saeed MS, Seyed-Yazdi J, Hekmatara H. Fe2O3/Fe3O4/PANI/MWCNT nanocomposite with the optimum amount and uniform orientation of Fe2O3/Fe3O4 NPs in polyaniline for high microwave absorbing performance. Journal of Alloys and Compounds. 2020;843. <URL>

25. Paul SJ, Gupta BK, Chandra P. Probing the electrical and dielectric properties of polyaniline multi-walled carbon nanotubes nanocomposites doped in different protonic acids. Polymer Bulletin. 2021;78:5667-83. <URL>

26. Wu T-M, Lin Y-W. Doped polyaniline/multi-walled carbon nanotube composites: Preparation, characterization and properties. Polymer. 2006;47(10):3576-82. <URL>

27. Phang SW, Tadokoro M, Watanabe J, Kuramoto N. Synthesis, characterization and microwave absorption property of doped polyaniline nanocomposites containing TiO2 nanoparticles and carbon nanotubes. Synthetic Metals. 2008;158(6):251-8. <URL>

28. Endo M, Takeuchi K, Hiraoka T, Furuta T, Kasai T, Sun X, et al. Stacking nature of graphene layers in carbon nanotubes and nanofibres. Journal of Physics and Chemistry of Solids. 1997;58(11):1707-12. <URL>

29. Zhang X, Zhang J, Liu Z. Tubular composite of doped polyaniline with multi-walled carbon nanotubes. Applied Physics A. 2005;80:1813-7. <URL>

30. Konyushenko EN, Stejskal J, Trchova M, Hradil J, Kovarova J, Prokes J, et al. Multi-wall carbon nanotubes coated with polyaniline. Polymer. 2006;47(16):5715-23. <URL>

31. Lefrant S, Baltog I, de la Chapelle ML, Baibarac M, Louarn G, Journet C, et al. Structural properties of some conducting polymers and carbon nanotubes investigated by SERS spectroscopy. Synthetic metals. 1999;100(1):13-27. <URL>

32. Li Y, Peng H, Li G, Chen K. Synthesis and electrochemical performance of sandwich-like polyaniline/graphene composite nanosheets. European Polymer Journal. 2012;48(8):1406-12. <URL>

33. Cochet M, Maser WK, Benito AM, Callejas MA, Martinez MT, Benoit JM, et al. Synthesis of a new polyaniline/nanotube composite: "in-situ" polymerisation

and charge transfer through site-selective interaction. Chemical Communications. 2001(16):1450-1. <URL>

34. Ghatak S, Chakraborty G, Meikap A, Woods T, Babu R, Blau W. Synthesis and characterization of polyaniline/carbon nanotube composites. Journal of Applied Polymer Science. 2011;119(2):1016-25. <URL>

35. Pekdemir ME, Kök M, Qader IN, AYDOĞDU Y. Preparation and physicochemical properties of mwcnt doped polyvinyl chloride/poly (ε-caprolactone) blend. Journal of Polymer Research. 2022;29(4):109. <URL>

36. Haruna H, Pekdemir ME, Tukur A, Coşkun M. Characterization, thermal and electrical properties of aminated PVC/oxidized MWCNT composites doped with nanographite. Journal of Thermal Analysis and Calorimetry. 2020;139:3887-95. <URL>

37. Heeger AJ. Nobel Lecture: Semiconducting and metallic polymers: The fourth generation of polymeric materials. Reviews of Modern Physics. 2001;73(3):681-700. <URL>

38. Bhadra S, Khastgir D, Singha NK, Lee JH. Progress in preparation, processing and applications of polyaniline. Progress in Polymer Science. 2009;34(8):783-810. <URL>

39. Wallace G, Spinks G, Teasdale P. Conductive electroactive polymers, Technomic Pub. Co. Inc, USA. 1997:107-25.

40. Zengin H, Zhou W, Jin J, Czerw R, Smith Jr DW, Echegoyen L, et al. Carbon nanotube doped polyaniline. Advanced materials. 2002;14(20):1480-3. <URL>

41. Virji S, Kaner RB, Weiller BH. Hydrogen sensors based on conductivity changes in polyaniline nanofibers. The Journal of Physical Chemistry B. 2006;110(44):22266-70. <URL>